

# THEORETICAL AND EXPERIMENTAL ANALYSIS OF THE ELECTRICAL HEATING OF SHAPE MEMORY ALLOY WIRES INTO A POLYMERIC MATRIX

Lorena Monteiro Cavalcanti Barbosa, [asukamonteiro@yahoo.com.br](mailto:asukamonteiro@yahoo.com.br)

Celso Rosendo Bezerra Filho, [celso@dem.ufcg.edu.br](mailto:celso@dem.ufcg.edu.br)

Carlos José de Araújo, [carlos@dem.ufcg.edu.br](mailto:carlos@dem.ufcg.edu.br)

Rômulo Pierre Batista dos Reis, [soromulo@hotmail.com](mailto:soromulo@hotmail.com)

Federal University of Campina Grande, Center of Science and Technology, Department of Mechanical Engineering, ZipCode 58429-900, Campina Grande, Paraíba, Brazil

**Abstract.** *The study of smart materials and structures has been extensively exploited in recent decades, due to their extraordinary properties. Among the smart materials, the shape memory alloys (SMA) are the best representatives of the class of metals. In this context, Ni-Ti SMA are the most successful smart metals today because combine good functional properties with a high mechanical strength. The electrical resistivity of Ni-Ti is high enough for direct Joule heating by passing an electrical current. This is an additional advantage as the activation of Ni-Ti SMA based devices is simplified. In this sense, this work presents a numerical and experimental investigation on the influence of electrical heating of Ni-Ti SMA wires embedded into a polymeric matrix. For this, a specific experimental set-up was employed and numerical simulation was developed using ANSYS CFX software. Experimental results approach the theoretical behavior of temperature distribution, mainly during heating of Ni-Ti wires. The results of cooling of the resin when decrease electrical current was not exactly precise but the qualitative behavior of temperature distribution as function of time were the same.*

**Keywords:** *Shape Memory Alloys, Joule heating, Ni-Ti, CFX, Active Composites.*

## 1. INTRODUCTION

The study of smart materials has been extensively exploited in recent decades, due to their extraordinary properties. These materials, commonly used as sensors and actuators in smart structures, have the ability to change shape, stiffness, natural frequencies, among others mechanical and physical properties, through the imposition of magnetic fields, temperature, voltage and others (Savi *et al.*, 2002; Ashrafiuon *et al.*, 2006; Wang, *et al.* 2006). Some materials of interest in the development of smart structures are piezoelectric crystals, electrostrictive, and magnetostrictive materials, shape memory alloys (SMA), electrorheological and magnetorheological fluids, and optical fibers (Culshaw, 1996; Srinivasan and McFarland, 2001).

Metallic alloys that exhibit the shape memory effect (SME) are materials that after undergoing an apparently permanent deformation are able to recover its original shape by a moderate heating. These materials can be easily deformed in a plastic way, at a relatively low temperature, but when heated can return the shape prior to deformation produced (Tanaka *et al.*, 2002). When the SME occurs only on heating, the phenomenon is designated as one-way shape memory effect. If this behavior is also observed during cooling, the designation of double or reversible shape memory effect (two-way shape memory effect) is used (Urbina *et al.*, 2010).

Another phenomenon that is very particular of the SMA is pseudoelasticity or superelasticity. It corresponds to a unique ability of recover large strains (up to 10%) when heated above a certain characteristic temperature, called the austenite finish temperature ( $A_f$ ), and submitted to mechanical loading (Meng *et al.*, 2004; Roh *et al.* 2006; Ibrahim *et al.*, 2009). In this behavior, by applying a mechanical load, the material behaves elastically until a critical stress is reached when, then, is initiated a plateau where the stress remains practically constant (Li *et al.* 2007). By unloading the SMA, the material returns to the starting point before being deformed. This behavior does not exist in the stress-strain diagram of a classic metal. It is noteworthy that there is a limit to the recovery of these strains represented by the elastic limit of the product phase, from which the material starts to behave plastically and the deformation can no longer be recovered.

The SMA have been quite promising for the development of control systems for attenuation of mechanical vibrations, allowing the system configuration much lighter, compact and efficient compared to traditional solutions (Huang, 2002). The use of SMA is a major scientific and technological challenge in the area of smart materials and structures. Currently there is a very large variety of materials presenting the SMA phenomenon (Humbecck, 2001; Chen, *et al.*, 2009; Kang *et al.*, 2011). However, only have commercial interest those with a significant shape recovery or that offer considerable recover forces when restricted to recovering its original shape after the imposition of temperature, for example, like as Ni-Ti and Ni-Ti based ones (hereinafter, called Ni-Ti SMA) (Frenzel *et al.*, 2004; Li *et al.* 2005).

The resistivity of Ni-Ti is high enough for direct Joule heating by passing an electrical current. This is an additional advantage as the actuation of SMA based devices is simplified (Frenzel *et. al.*,2011). In terms of the size of Ni-Ti SMA in engineering applications, one can see a quick movement in recent years from large size (An *et al.*, 2008).

The structure to be studied in this work is a Shape Memory Alloy Hybrid Composite (SMAHC) designed as an active beam of epoxy resin that contains five Ni-Ti pre-trained wire actuators, uniformly distributed along its neutral plane. These SMA wires can be activated differently and controlled by resistive heating (Joule effect). This work was conducted in two different ways: experimentally and by numerical simulation.

In this sense, this paper aims to show the temperature distribution as a function of the electrical current, when only one Ni-Ti SMA wire is driven into epoxy beam, and to compare the results of numerical simulation with some experiments.

## 2. MATERIAL AND METHODS

### 2.1 The SMAHC Beam

The system in analysis is a SMAHC beam with 300 x 24 x 4 mm with Ni-Ti SMA wires of 0.29 mm in diameter and 300 mm in length. Figure (1) shows a schematic drawing of SMAHC and photography of the real system. For this analysis only one Ni-Ti wire (that the center) is driven by an electrical current waveform that varies from 0 to 1.5 A during heating and from 1.5 A to 0 A during cooling. These trained Ni-Ti SMA wires, when heated electrically, tends to shrink inside the composite. In this first work this effect will not be considered. Properties of the epoxy resin and Ni-Ti wires shown in Tab. (1) are considered constant.

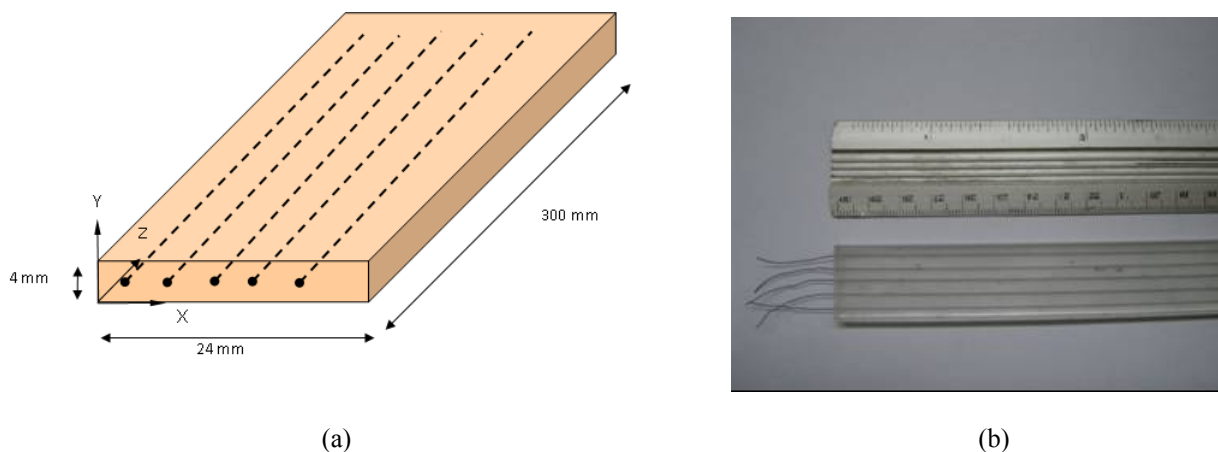


Figure 1. The SMAHC beam with Ni-Ti SMA wires. (a) Schematic drawing. (b) Photo of the real SMAHC.

Table 1. Material properties of epoxy resin and Ni-Ti wires.

| Properties                   | Epoxy | Ni-Ti Wire |
|------------------------------|-------|------------|
| Density (g/cm <sup>3</sup> ) | 1.18  | 6.48       |
| Reference Pressure (atm)     | 1     | 1          |
| Reference Temperature (°C)   | 24    | 24         |
| Resistivity (μΩ.m)           | -     | 85         |
| Thermal Conductivity (W/m.K) | 0.4   | 8.5        |
| Specific Heat (J/kg.K)       | 1050  | 400        |

### 2.2 Experimental Set-up

As pointed out in Fig. (2), the SMAHC beam was assembled in a single cantilever beam way to verify the effect of electrical activation when different Ni-Ti wires are activated by heating and cooling. The specific activation mode employed is represented in Fig. (3). The temperature of the SMAHC was measured at three different points along the

neutral plane of the beam using micro-thermocouple type K with 80  $\mu\text{m}$  in diameter, placed close to the Ni-Ti wires. Resistive heating of the central Ni-Ti SMA is done by a programmable power supply (Agilent, E3633A model) that generates the triangular electrical current waveform. The temperatures in the beam and the electrical resistance of Ni-Ti wires were stored in a data acquisition system (Agilent, 34970A model).

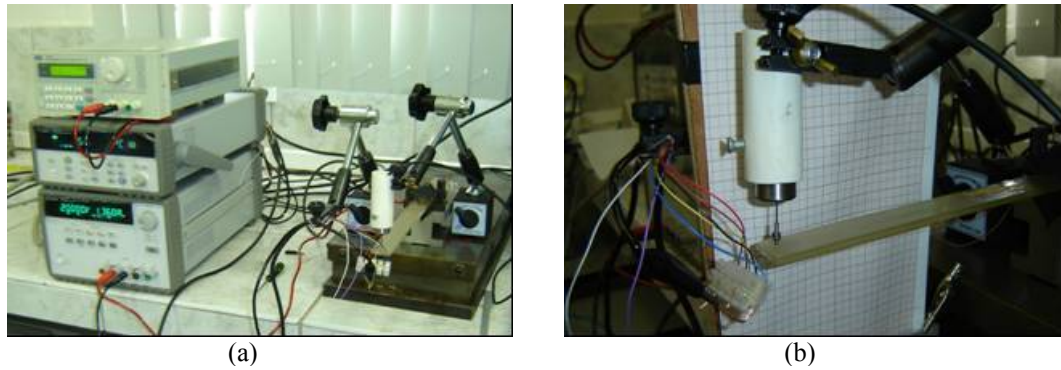


Figure 2. Experimental test bench. (a) General view. (b) Detailed view of the SMAHC.

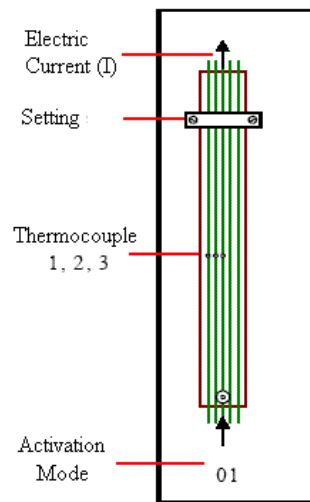


Figure 3. Electrical activation of the central Ni-Ti SMA wire.

### 2.3 Numerical Analysis

Commercial *ANSYS CFX 5.6* software was used to simulate the heat conduction when only the central Ni-Ti SMA wire was electrically activated, as shown in Fig. (3). The tri-dimensional model employed comprises the energy conservation equation in three directions.

A transient model was used with time step of 1s for a total time of 260s, and a convergence criterion of  $10^{-7}$ . The mesh was built in *CFX-Build*, with two domains: SMAHC beam and Ni-Ti wires. Figures (4) and (5) show the volume and cross-section distributions of the mesh and computational domain.

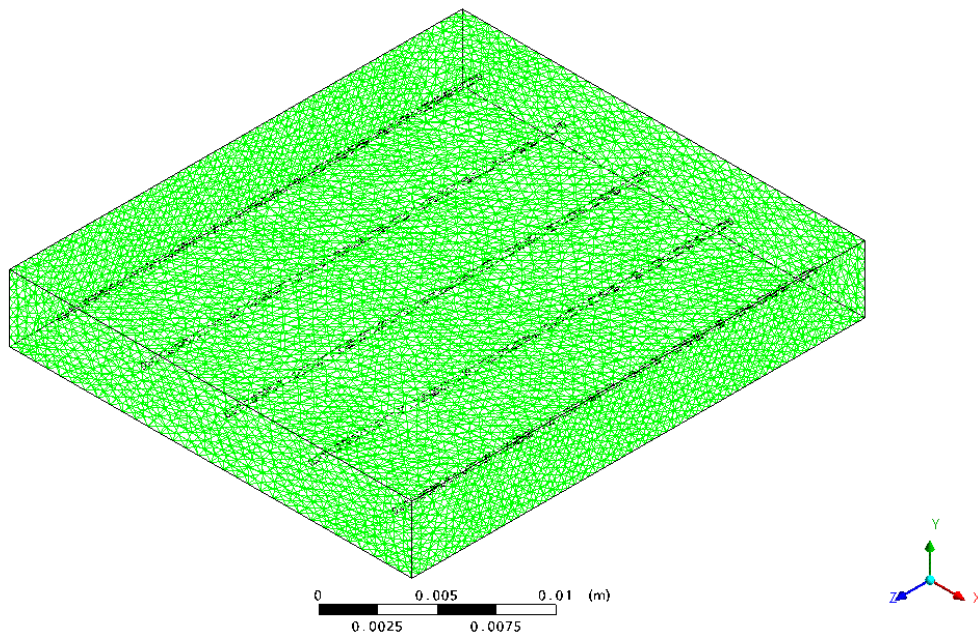


Figure 4. Volume distribution of the mesh in the SMAHC beam with Ni-Ti wires (isometric view).

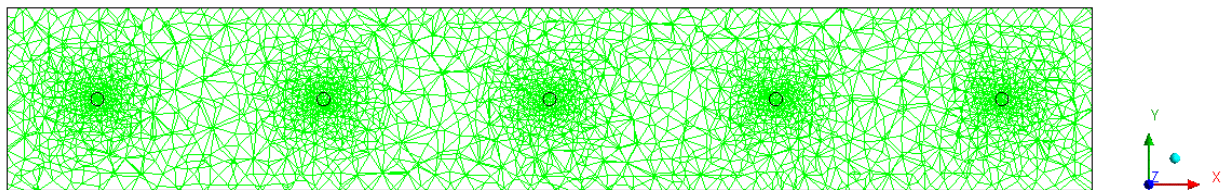


Figure 5. Cross-section distribution of the mesh in the SMAHC beam with Ni-Ti wires (XY Plane).

### 2.3.1. Mathematical equations

The proposed problem can be described by Eq. (1):

$$\frac{\partial \rho h_{hot}}{\partial t} - \frac{\partial p}{\partial t} + \nabla \bullet (\rho U h_{hot}) = \nabla \bullet (\lambda \nabla T) + S_E \quad (1)$$

where  $U$  is the flow velocity;  $S_E$  is the source force,  $\rho$  is the density,  $\lambda$  is the thermal conductivity,  $p$  is the static pressure,  $T$  is the temperature, and  $h_{hot}$  is the total enthalpy, related to the static enthalpy  $h(T,P)$  by Eq. (2):

$$h_{hot} = h + \frac{1}{2} U^2 \quad (2)$$

where  $h$  is the specific static enthalpy.

## 3. RESULTS

Figures (6) and (7) show the behavior of temperature distribution as a function of electrical current when the central Ni-Ti wire is driven. The presented results were obtained for the  $(x,y,z)$  point corresponding to  $(12\text{mm}, 2.375\text{mm}, 128\text{mm})$ , for both experimental and computational results. In this case, the temperature increases and decreases when electrical current varies linearly from 0 to 1.5 A and from 1.5 A to 0.

As can be verified in Fig. (6), for experimental measurements the temperature varies from 23.8 °C, when electrical current is low (0.07 A), until 65.7°C, for maximum current (1.5 A). The computational results are very similar, when electrical current is 1.5 A the maximum temperature is about 63.3 °C.

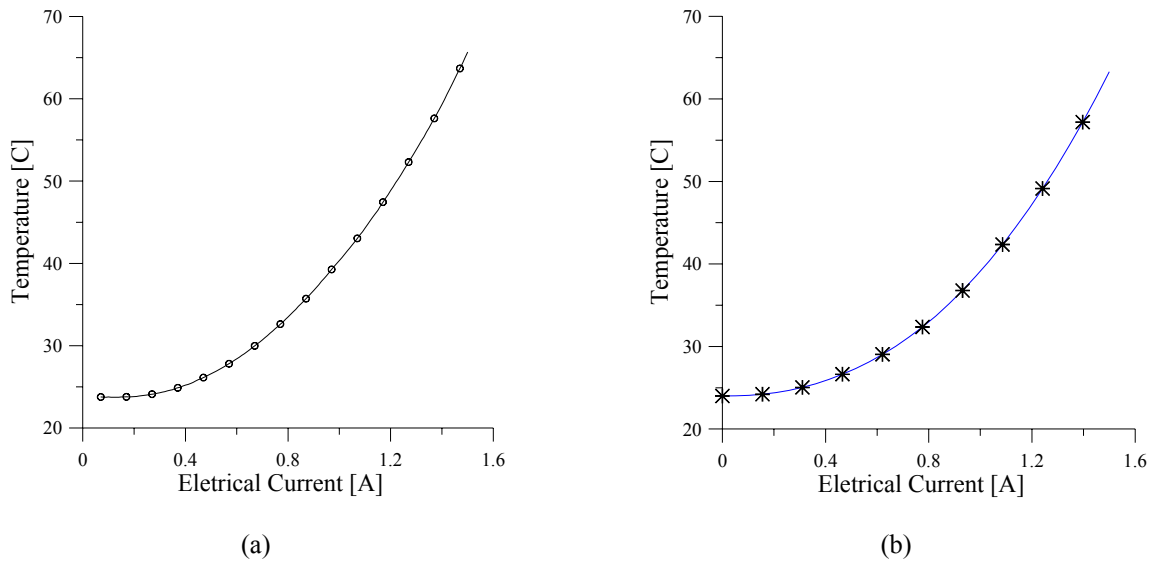


Figure 6. Temperature as a function of electrical current during heating. (a) Experimental results. (b) Numerical Simulation.

Figure (7) shows that temperature still increase even with reduction in electrical current (for cooling), and reaches a maximum of 68.8 °C for 1.3 A in the experimental measurements and 65.4°C for computational simulation.

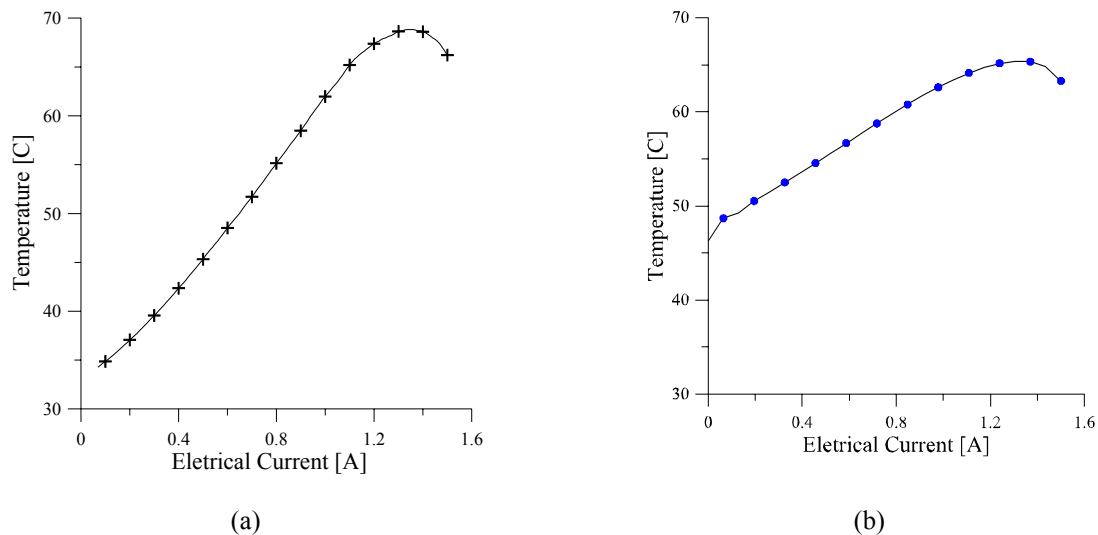


Figure 7. Temperature as function of electrical current during cooling. (a) Experimental results. (b) Numerical Simulation.

Figure (7) has showed some discrepancy in the values of cooling of the SMAHC beam. For experimental measurements it is observed a great loss of heat when the current is reduced and when the current attains 0 A the temperature reaches 34.2 °C, while for the computational simulation this temperature is 46.3 °C.

The behavior of temperature distribution along the cross section of the SMAHC beam (XY plane for  $z = 128$  mm) is shown in Figs. (8) and (9), through the contour lines. Figure (8) shows this thermal distribution when electrical current increases while Fig. (9) shows this behavior when electrical current decreases.

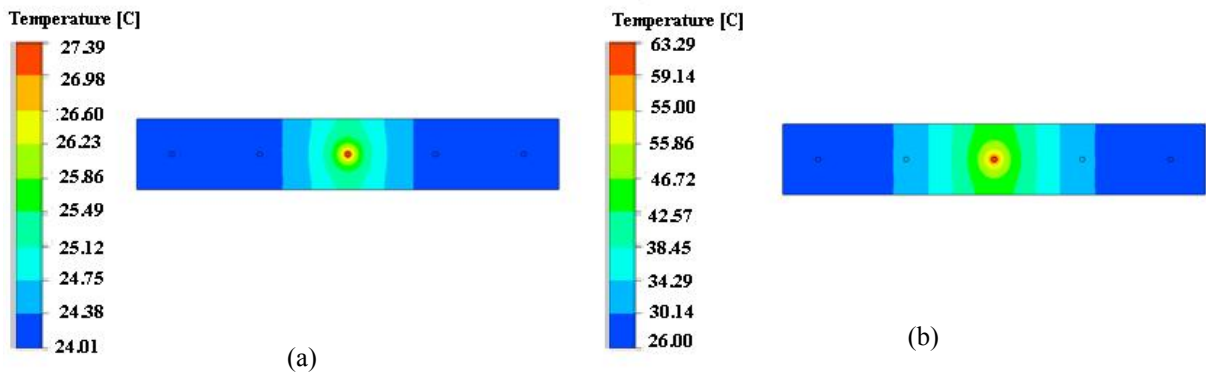


Figure 8. Temperature distribution in the cross-section of the SMAHC during increase of electrical current. (a) 0.5 A. (b) 1.5 A.

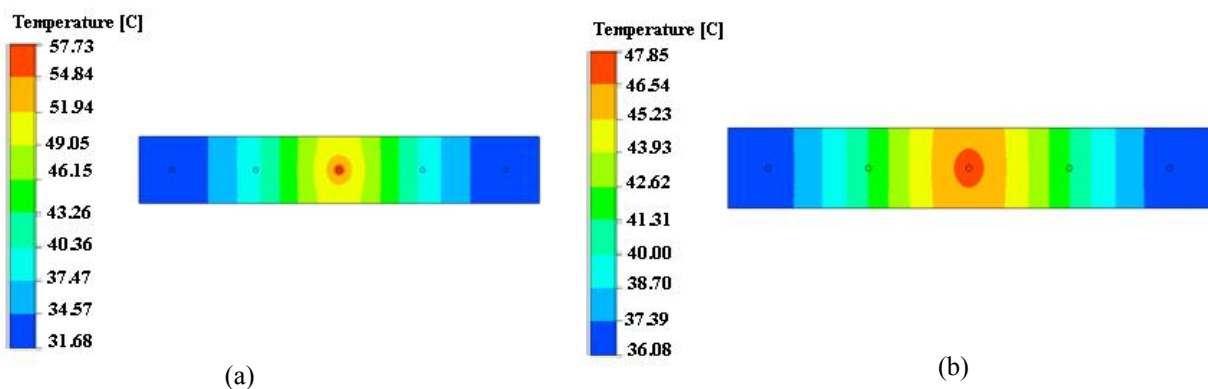


Figure 9. Temperature distribution in the cross-section of the SMAHC during reduction of electrical current. (a) 0.6 A. (b) 0 A.

Similar thermal behaviors are shown in Fig. (10) for the XZ plane during increase and decrease of electrical current. In this figure it is clear how the activation of the central Ni-Ti wire was done and how the temperature distribution along the length of the SMAHC occurs.

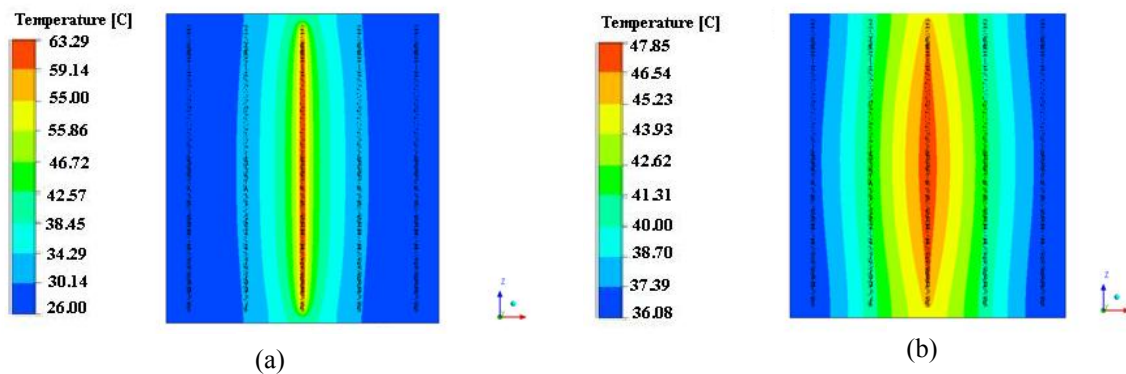


Figure 10. Temperature distribution along the XZ plane of the SMAHC. (a) During current increase ( $I = 1.5$  A). (b) During current decrease ( $I = 0$  A).

#### 4. CONCLUSIONS

Numerical simulation and experimental measurements concerning the thermal distribution in the volume of a SMAHC with electrical activation by a central Ni-Ti wire were consistent. The best concordance between numerical and experimental results were observed for the heating stage, when electrical current increases from 0 A to 1.5 A. For electrical current decrease from 1.5 to 0 A, it was verified a considerable discrepancy, mainly when the current becomes smaller than 0.6 A. However, the qualitative behavior of temperature distribution is similar for experimental and numerical results. This discrepancy can be caused by several problems, as the fact that the point where experimental

and numerical results are examined could not be exactly the same and numerical simulation doesn't consider the phase transformation of the Ni-Ti SMA wires.

## 5. ACKNOWLEDGEMENTS

The authors thank the Conselho Nacional de Desenvolvimento Científico e Tecnológico (CNPq), Brazilian office, for sponsoring the INCT of Smart Structures in Engineering (INCT grant 574001/2008-5) during the course of these investigations.

## 6. REFERENCES

- An L., Huang W.M., Fu Y.Q., Guo N.Q., 2008. "A note on size effect in actuating NiTi shape memory alloys by electrical current". *Materials & Design*, Vol.29, pp.1432-1437.
- Ashrafiuon H., Eshraghi M., and Elahinia M.H., 2006. "Position Control of a Three-link Shape Memory Alloy Actuated Robot". *Journal of Intelligent Material Systems and Structures*, Vol. 17, pp 381-392.
- Chen J., Lia Z., Zhaoc Y.Y., 2009. "A high-working-temperature CuAlMnZr shape memory alloy". *Journal of Alloys and Compounds* vol. 480, PP. 481–484.
- Culshaw, B., 1996. "Smart Structures and Materials". Artech House Optoelectronic Library, England.
- Frenzel J., Burow J. A., Payton E. J., Rezanka S. and Eggeler G., 2011. "Improvement of NiTi Shape Memory Actuator Performance Through Ultra-Fine Grained and Nanocrystalline Microstructures". *Advanced Engineering Materials*, Vol.12, No. 4, pp. 256–268.
- Frenzel J., Zhang Z., Neuking K., Eggeler G., 2004. "High quality vacuum induction melting of small quantities of NiTi shape memory alloys in graphite crucibles". *Journal of Alloys and Compounds*, Vol.385, pp. 214–223 .
- Huang W., 2002. "On the selection of shape memory alloys for actuators". *Materials & Design*, Vol. 23, pp.11-19.
- Humbeek J. V., 2001. "Shape Memory Alloys: A Material and a Technology". *Advanced Engineering Materials* 2001, vol. 3, No. 11. pp 837-850.
- Ibrahim H. H., Tawfik M. and Negm H. M., 2009. "Limit-Cycle Oscillation of Shape Memory Alloy Hybrid Composite Plates at Elevated Temperatures". *Mechanics of Advanced Materials and Structures*, Vol. 16, pp. 429-441.
- Kang H., Wu S., Wu L., 2011. "3R and 14M martensitic transformations in as-rolled and annealed Ni64Al34.5Re1.5 shape memory alloy". *Journal of Alloys and Compounds* Vol. 509, pp. 1619–1625.
- Li L., Qingbin L., Zhang F., 2007. "Behavior of Smart Concrete Beams with Embedded Shape Memory Alloy Bundles". *Journal of Intelligent Material Systems and Structures*, Vol. 18, pp.1003-1014.
- Li Y., Rong L., Wang Z., Qi G., Wang C., 2005. "Temperature memory effect of Ti50Ni30Cu20 (at.%) alloy". *Journal of Alloys and Compounds*. Vol. 400, pp. 112–115.
- Meng X.L., Zheng Y.F., Cai W., Zhao L.C, 2004. "Two-way shape memory effect of a TiNiHf high temperature shape memory alloy". *Journal of Alloys and Compounds*. Vol. 372, pp. 180–186.
- Roh J., Han J. and Lee I., 2006. "Nonlinear Finite Element Simulation of Shape Adaptive Structures with SMA Strip Actuator". *Journal of Intelligent Material Systems and Structures*, Vol. 17: 1007-1022
- Savi M. A., Paiva A., Bae^ta-neves A. P., Pacheco P. M. C. L., 2002. "Phenomenological Modeling and Numerical Simulation of Shape Memory Alloys: A Thermo-plastic-phase Transformation Coupled Model". *Journal of Intelligent Material Systems and Structures*, Vol. 13, pp.261-273.
- Srinivasan, A.V., McFarland, D.M., 2001. *Smart Structures – Analysis and Design*, Cambridge University Press, Cambridge, UK.
- Tanaka K., Ohnami D., Watanabe T., Kosegawa J., 2002. "Micromechanical simulations of thermomechanical behavior in shape memory alloys: transformation conditions and thermomechanical hysteresis". *Mechanics of Materials*, Vol. 34, pp. 279-298.
- Urbina C., Flor S. De la, Ferrando F., 2010. "R-phase influence on different two-way shape memory training methods in NiTi shape memory alloys". *Journal of Alloys and Compounds*. Vol. 490, pp. 499–507.
- Wang G., Yang G., Huang Y, Wang Y, 2006. "Effect of Heat Treatment and Thermochemical treatment on Linear Recovery Property of TiNi Shape Memory Alloy". *Advanced Engineering Materials*, Vol. 8, pp. 107-111.

## 7. RESPONSIBILITY NOTICE

The authors are the only responsible for the printed material included in this paper.